Journal of Clinical Immunology (2019) 39:401–413
https://doi.org/10.1007/s10875-019-00629-0

ORIGINAL ARTICLE

Novel *MALT1* Mutation Linked to Immunodeficiency, Immune Dysregulation, and an Abnormal T Cell Receptor Repertoire

Shirly Frizinsky[1] · Erez Rechavi[1] · Ortal Barel[2] · Rose H. Najeeb[3] · Shoshana Greenberger[4,5] · Yu Nee Lee[1,2] · Amos J. Simon[1,2] · Atar Lev[1,2] · Chi A. Ma[6] · Guangping Sun[6] · Sarah A. Blackstone[6] · Joshua D. Milner[6] · Raz Somech[1,2,4] · Tali Stauber[1,2,4]

Received: 16 October 2018 / Accepted: 9 April 2019 / Published online: 29 April 2019

Abstract

MALT1 (mucosa-associated lymphoid tissue lymphoma-translocation gene 1) is an intracellular signaling protein that activates NFκB and is crucial for both the adaptive and innate immune responses. Only 6 patients with immune deficiencies secondary to inherited mutations in the *MALT1* gene have been described.

Purpose

To provide clinical and immunological insights from 2 patients diagnosed with MALT1 immunodeficiency syndrome due to a novel *MALT1* mutation.

Methods

Two cousins with suspected combined immunodeficiency underwent immunological and genetic work-up, including lymphocyte phenotyping, lymphocyte activation by mitogen stimulation, and next-generation sequencing (NGS) of T cell receptor gamma chain (TRG) repertoire. Whole exome sequencing was performed to identify the underlying genetic defect.

Results

Clinical findings included recurrent infections, failure to thrive, lymphadenopathy, dermatitis, and autoimmunity. Immune work-up revealed lymphocytosis, low to normal levels of immunoglobulins, absence of regulatory T cells, and low Th17 cells. A normal proliferative response was induced by phytohemagglutinin and IL-2 but was diminished with anti-CD3. TRG repertoire was diverse with a clonal expansion pattern. Genetic analysis identified a novel autosomal recessive homozygous c.1799T>A; p.I600N missense mutation in *MALT1*. MALT1 protein expression was markedly reduced, and in vitro IL-2 production and NFκB signaling pathway were significantly impaired.

Conclusions

Two patients harboring a novel *MALT1* mutation presented with signs of immune deficiency and dysregulation and were found to have an abnormal T cell receptor repertoire. These findings reinforce the link between MALT1 deficiency and combined immunodeficiency. Early diagnosis is crucial, and curative treatment by hematopoietic stem cell transplantation may be warranted.

Keywords Autoimmunity · combined immunodeficiency (CID) · MALT1 · NGS · regulatory T cells · TCR repertoire · immune dysregulation · NFκB

✉ Raz Somech
raz.somech@sheba.health.gov.il

[1] Pediatric Department A and the Immunology Service, Jeffrey Modell Foundation Center, Edmond and Lily Safra Children's Hospital, Sheba Medical Center, 52621 Tel Hashomer, Israel

[2] The Wohl Institute for Translational Medicine and Cancer Research Center, Sheba Medical Center, Tel Hashomer, Israel

[3] Pediatric Department, Makassed Hospital, Jerusalem, Israel

[4] Sackler Faculty of Medicine, Tel Aviv University, Tel Aviv, Israel

[5] Department of Dermatology, Sheba Medical Center, Tel Hashomer, Israel

[6] Laboratory of Allergic Diseases, National Institute of Allergy and Infectious Diseases, Bethesda, MD, USA

Abbreviations

CBM	CARD9/10/11-BCL10-MALT1
CID	combined immunodeficiency
HSCT	hematopoietic stem cell transplantation
MALT-1	mucosa-associated lymphoid tissue lymphoma-translocation gene 1
NGS	next-generation sequencing
PBMCs	peripheral blood mononuclear cells
SCID	severe combined immunodeficiency
TRECs	T cell receptor excision circles
TCR	T cell receptor

Introduction

Identification of the genetic causes underlying human primary immunodeficiency (PID) is critical to understanding disease pathogenesis, diagnosis, and treatment of affected patients [1, 2]. The most unfavorable PID is severe combined immunodeficiency (SCID), affecting both T and B cells and, in some cases, NK cells [3]. While SCID diagnosis is clearly defined, there is a much larger group of patients diagnosed with an undefined combined immunodeficiency (CID). These patients present similarly to those with SCID, but, in contrast, have circulating T cells. Unlike SCID patients, CID patients can survive beyond the first year of life without immune restoration [4]. In addition to their susceptibility to infections, CID patients can present with lymphoproliferative disease, autoimmunity, atopy, and enteropathy [4–6]. The characteristic immunological profile of these patients is one of profound T cell dysfunction with abnormal cellular and humoral immunity [3, 4]. Diagnosing CID is challenging due to the wide variety of clinical presentations and spectrum of T cell dysfunction. As a result, clinical decision-making, specifically with regard to hematopoietic stem cell transplantation (HSCT), is especially difficult.

A prime example of an inborn error of immunity that causes CID results from mutation of the mucosa-associated lymphoid tissue lymphoma-translocation gene 1 (*MALT1*). Jabara et al. [7] and McKinnon et al. [8] first reported mutations in this gene, and, since then, only a few cases were added to the literature [9, 10]. MALT1, a part of the CBM complex (CARD11/BCL-10/MALT1), is a caspase-like cysteine protease essential for NFκB activation [11–14]. The MALT1 protein has two major activities. First, it acts as a scaffold, recruiting different proteins in the NFκB signaling pathway. Additionally, it serves as a cardinal protease, regulating NFκB activity by cleaving various substrates [15, 16]. T and B cell receptor (TCR) activation results in recruitment of the CBM complex, which in turn leads to the ubiquitination of NEMO (NFκB essential modulator). This activates the IkB kinase (IKK) complex, thereby enabling NFκB to undergo nuclear translocation and initiate gene transcription necessary for cellular activation, including IL-2 secretion. Due to the central role of the MALT1 protein in this cascade, mutations in the encoding gene significantly compromise NFκB activity [11]. Other pathways, such as mTORC1, may also depend on the CBM complex [17]. The current understanding of MALT1 deficiency is far from complete. Our knowledge of this genetic deficiency arises from the handful of cases reported to date, which were heterogeneously characterized by recurrent systemic infections, dermatitis, inflammatory bowel disease, failure to thrive, and variable additional characteristics [7–10]. The immunological phenotype is similarly variable though is typically characterized by normal lymphocyte counts, normal or reduced immunoglobulin levels, low antibody titers following immunizations, and abnormal T cell response to mitogenic stimuli. Previous studies also demonstrated in vitro low IL-2 secretion following TCR stimulation [7, 9, 10], normal or reduced counts of T regulatory cells [8–10], and low counts of Th17 cells [8].

In this paper, we describe two related patients who presented with findings suggestive of CID, ultimately found to harbor a *MALT1* mutation not previously described. This research extends current understanding of *MALT1* mutations, specifically with regard to the associated clinical findings and resulting abnormal T cell development and activation.

Methods

Clinical Data

Patient information was obtained from the electronic medical record of our hospital. The guardians were interviewed, and the authors examined the patients. Informed consent was obtained, and all procedures were performed in accordance with the ethical standards of the institutional and/or national research committee and with the Helsinki declaration and its later amendments or comparable ethical standards.

Immune Function

Cell surface markers of peripheral blood mononuclear cells (PBMCs) were determined by immunofluorescent staining using flow cytometry (FACS, NAVIOS, Beckman Coulter) with antibodies purchased from Beckman Coulter. Lymphocyte proliferation was done in response to phytohemagglutinin and anti-CD3 (using tritiated thymidine incorporation). The cells were harvested three days after collection, and the samples were counted in a liquid scintillation counter. All assays were performed in triplicate, and a stimulation index was calculated as the ratio between stimulated and unstimulated lymphocyte responses. The resultant stimulation index was compared with the stimulation index obtained from

the normal controls. Serum concentration of immunoglobulins was measured by nephelometry.

Quantification of TRECs

TREC analysis was performed using DNA extracted from the study patients' PBMCs. The amount of signal joint TREC copies per DNA content was determined by real-time quantitative PCR. Reactions were performed using 0.5-mcg genomic DNA and PCRs contained in TaqMan universal PCR master mix (Applied Biosystems), specific primers (900 nM), and FAM-TAMRA probes (250 nM). RQ-PCR was carried out in StepOnePlus (Applied Biosystems). The number of TRECs in a given sample was estimated by comparing the cycle threshold value obtained with a standard curve obtained from PCRs performed with 10-fold serial dilutions of an internal standard. Amplification of RNAseP (Taq-Man assay, Applied Biosystems) served as a quality control to verify similar amounts of genomic DNA that were used in the assays.

PMA/Ionomycin Stimulation and Cytokine Production

PBMCs (1×10^6/mL) were incubated with 100 μM PMA and 1 μM ionomycin (Sigma-Aldrich) in 48-well plate, and GolgiStop (BD Biosciences) was added 1 h later. After 5 h stimulation, the PBMCs were fixed with paraformaldehyde and, then, permeabilized with methanol. Cell surface markers and cytokines were stained and analyzed by BD LSRFortessa.

TCR Repertoire

Representatives of specific TCR-Variable b families were detected and quantified using patients' PBMCs with flow cytometry (NAVIOS, Beckman Coulter) according to the manufacturer's instructions (Beta Mark TCR Vb repertoire kit, Beckman Coulter). Normal control values comprised of 58 healthy people were obtained from the kit.

Quantification of Th17 Cells

IL-17A T cells were evaluated by intracellular staining. Non-adherent PBMCs (prepared after the removal of adherent monocytes) were stimulated for 12 h with 40 ng/mL PMA (Sigma-Aldrich) and 10^{-5} M ionomycin (Sigma-Aldrich) in the presence of 1 μg/mL GolgiPlug (BD Biosciences). The cells were, then, harvested, and extracellular labeling was achieved by incubating the cells with anti-human CD3-PC7 (Beckman Coulter). Intracellular staining was done using the PerFix-nc kit (Beckman Coulter) and anti-human IL17-PB antibody (Beckman Coulter).

Analysis of T Regulatory Cells

Lymphocytes were obtained from the infants' peripheral blood by density gradient centrifugation on Lymphoprep™ (STEMCELL Technologies). For the detection of FOXP3, the cells were fixed and permeabilized using a FOXP3 staining buffer set according to the manufacturer's protocol (eBioscience). The antibodies used were CD4-FITC, CD25-PE (BD Biosciences), and FOXP3-APC (eBioscience). Cell samples were analyzed using fluorescence-activated cell sorting (FACS, NAVIOS, and Beckman Coulter) and the Kaluza software (Beckman Coulter).

Next-Generation Sequencing

TCR libraries were generated from patient and control genomic DNA extracted from PBMCs using primers for conserved regions of V and J genes in the *TRG* (TCR-gamma) locus according to the manufacturer's protocol (Lymphotrack; Invivoscibe Technologies®, Carlsbad, CA, USA). Quantified libraries were pooled and sequenced using MiSeq Illumina Technology®. FASTA files from the filtered sequences were submitted to ImMunoGeneTics (IMGT) HighV-QUEST webserver® (http://www.imgt.org), filtered for productive sequences only (no stop codons or frame shifts), and analyzed [18]. Analyses were performed on CDR3 amino acid sequences. For TCR repertoires, V and J gene usage patterns were analyzed. Repertoire diversity was calculated using Shannon and Gini-Simpson's diversity indices [19].

Exome Sequencing Analysis and SANGER Sequencing

High-throughput sequencing for whole exome sequencing was performed on genomic DNA samples extracted from PBMCs from patients 1 (P1) and 2 (P2), and coding regions were enriched with a SureSelect Human All Exon V5 Kit (Agilent) and, then, sequenced as 100-bp paired-end runs on an Illumina HiSeq 2500 (Illumina Inc.). We used the BWA mem algorithm (version 0.7.12) [20] for the alignment of the sequence reads to the human reference genome (hg19). The HaplotypeCaller algorithm of GATK version 3.4 was applied for variant calling, as recommended in the best practice pipeline [21]. KGG-seq v.08 was used for annotation of identified variants [22], and in-house scripts were applied for filtering, based on family pedigree and local dataset of variants detected in previous sequencing projects.

The *MALT1* mutation was validated by dideoxy Sanger sequencing in the patients and carriers. Data were evaluated using Sequencer v5.0 software (Gene Codes Corporation).

Western Blot Analysis

Western blot analysis was described previously [23]. The total PBMC was lysed in RIPA buffer, and the soluble fraction was heat-denatured in LDS sample buffer (Life Technologies) with 0.1 M DTT and loaded onto 4–12% Tris-Bis polyacrylamide gradient gel. Protein was transferred from gel to PVDF membrane and detected by MALT1 antibody (Cell Signaling Technology), β-actin, and HRP-conjugated secondary antibody.

Results

Clinical Description

We present two patients evaluated for suspected immunodeficiency. The patients were first cousins born to a highly consanguineous family of Palestinian origin (Fig. 1). Patient 1 (P1) was born to a pair of healthy second cousins. Birth was at term and uncomplicated. Shortly after birth, a recurrent pustular rash was noted. By the age of six months, he had suffered from recurrent episodes of pneumonia, cellulitis and abscesses, lymphadenitis, chronic intermittent diarrhea, and severe failure to thrive. He was referred to our hospital at the age of 11 months for further evaluation. His examination was notable for dysmorphic features with hypertrichosis, coarse facies, deep palmar creases bilaterally, and small toenails. A diffuse eczematous rash, multiple gluteal abscesses, onychomycosis, and generalized lymphadenopathy were also noted. Pneumonia was diagnosed clinically, and urine culture grew *Klebsiella pneumoniae*. Aspirate from an enlarged infected lymph node was positive for Methicillin-resistant *Staphylococcus aureus*. Cultures from oral lesions grew *HSV-1* and *Candida*. Following completion of initial antimicrobial therapy, P1 went on to develop numerous additional infections, including bacterial and viral respiratory infections, periorbital cellulitis, *Staphylococcus aureus* and non-typeable *Haemophilus influenza* bacteremia, herpetic skin infections, persistent herpetic kerato-conjunctivitis, and *Salmonella* and *Campylobacter* gastroenteritis. In addition, subsequent examination showed alopecia involving the scalp and eyebrows. Computed tomography of the chest and lungs demonstrated bilateral axillary lymphadenopathy with lung consolidation and ground glass appearance. Bronchoalveolar lavage showed no significant findings. Lymph node biopsy showed signs of a reactive process with no signs of neoplasia. Further lymphoproliferative, metabolic, and autoimmune investigations were all normal.

Patient 2 (P2) was born without complications to consanguineous healthy parents of Palestinian origin. Family history was notable for an older sibling who died at one year of age, apparently due to a severe infection. P2 initially presented at a few weeks of age to another institution and was treated there for recurrent severe infections, including pneumonia, meningitis, and urinary tract infections. Chronic diarrhea and oral thrush were also noted. The patient was referred to our institution at the age of 5 months for suspected immunodeficiency. Physical examination was notable for bronchiolitis, severe failure to thrive, seborrheic dermatitis, onychomycosis, and vitiligo. Infectious work-up demonstrated positive whole blood PCR for CMV, and nasal swabs were positive for influenza and parainfluenza viruses on PCR. Chest X-ray demonstrated bilateral alveolar infiltrates, with a normal-sized

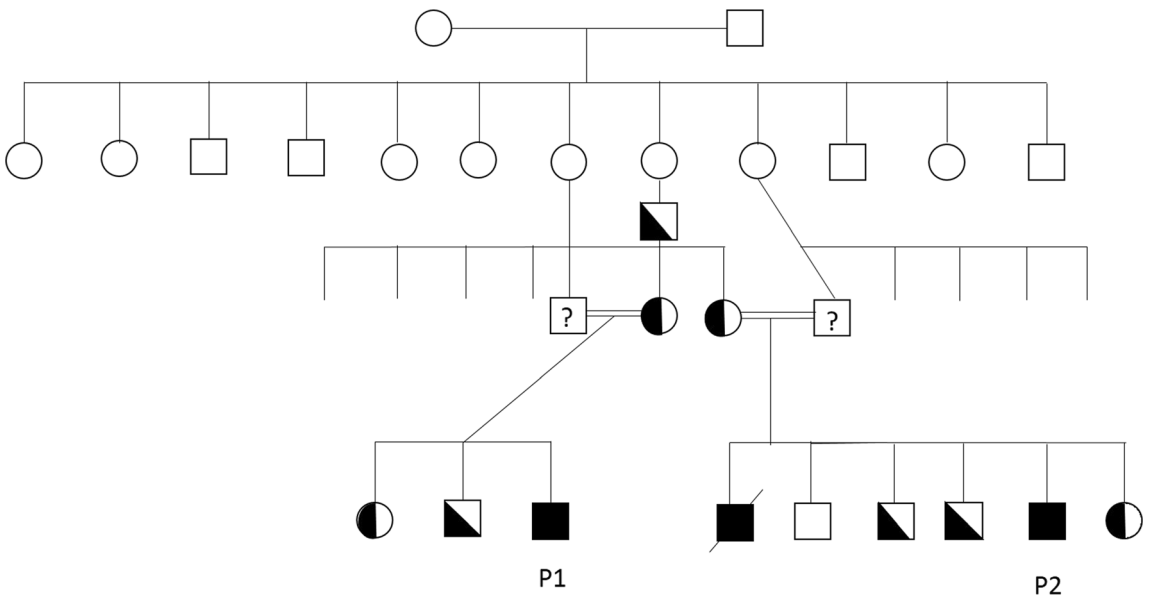

Fig. 1 Pedigree of P1 and P2's family. Double lines indicate consanguinity (first-degree cousins); filled black circles or squares depict the patients; half-filled black circles or squares depict carrier state; diagonal lines indicate deceased individuals

mediastinum, and abdominal ultrasound was normal with no evidence for hepatosplenomegaly. As with his cousin, further lymphoproliferative, metabolic, and autoimmune investigations were all normal.

Currently, both patients are stable on intravenous immunoglobulin (IVIG) replacement therapy and antibiotic prophylaxis, awaiting HSCT.

Immunological Evaluation

The initial immunologic investigation for both patients revealed leukocytosis with lymphocytosis and eosinophilia (Table 1). Immunoglobulin levels were initially within normal range, but, over time, P1 developed hypogammaglobinemia and required monthly IVIG replacement therapy. Post-immunization titers (HBV and poliovirus vaccine) were undetectable for P1 and within normal ranges for P2. Neutrophil function studies did not show any abnormality in chemotaxis or oxidative burst. Immunophenotyping of lymphocytes showed normal representation of T, B, and NK cells. Surprisingly, P1 had an elevated fraction of double-negative T cells (CD3+$\alpha\beta$+ CD4–CD8–) (Table 1). In both patients, there was an absence of T regulatory cell expression (C3+ CD4+CD25+Foxp3+) and a decrease in the percentage of Th17 cells. B cell subsets (Table 1) revealed low percentage of marginal zone B cells (IgD+CD19+CD27+) and high percentage of transitional B cells (IgM++CD19+CD38++) compared to control (3.5% vs. 4.1–13.9% and 31% vs. 3.3–16.5%, respectively). Lymphocyte proliferation test (Table 2) for both patients was normal following stimulation with phytohemagglutinin (PHA) and IL-2 but markedly reduced following stimulation with anti-CD3. P2's PBMCs demonstrated decreased IL-2 expression following stimulation with PMA and ionomycin (Fig. 2). In order to evaluate thymus activity and naïve T cell production, T cell receptor excision circles (TRECs) were quantified for both patients. In both patients, TREC levels were within normal ranges (Table 1). The TCR repertoire was assessed with the traditional TCR-Vβ assay using flow cytometry. P2 had a completely normal repertoire whereas P1 had overexpression of TCR (vβ 7.1) with an otherwise normal repertoire compared to healthy controls (Fig. 3).

Next-Generation Sequencing

In order to further characterize the TCR repertoire, high-throughput immune sequencing of the TRG (T cell receptor γ chain) repertoire was performed on PBMCs from both patients and a healthy age-matched control. Of the four chains of TCR (α, β, γ, δ), the TRG repertoire was specifically selected for sequencing for the following reasons: it is rearranged earlier in the development of T cells; it is often used for sensitive and comprehensive detection of clonal expansions [24–26], and because of the prominent role of γδT cell in skin immunity [26, 27].

As shown in Fig. 4a, both patients expressed a diverse repertoire with evidence of clonal expansion. We used Shannon's H and Simpson's D indices [19] to measure the diversity of the repertoires, which are commonly used in ecology [28, 29]. These diversity indices take into account the unique and total sequences and the evenness of the clonal size. Thus, the Shannon's H index reflects the overall diversity of the repertoire whereas the Simpson's D index focuses on how unevenly the clones are distributed in a given repertoire due to presence of clonal expansions, as was previously shown [30, 31]. The Shannon's H diversity index for both patients' repertoires was relatively low compared with the controls (Fig. 4b). Calculation of the Simpson's D index showed moderate unevenness in the TRG repertoire for the patients as compared to the controls (Fig. 4b).

We also analyzed the total and unique number of sequences of the TRG repertoire. In general, the unique number of sequences portrays the number of clones that develop in the thymus and are released into the peripheral blood, while the total number of sequences reflects the absolute number of γδ T cells in the peripheral blood. While the unique number of sequences of the patients did not differ from that of the controls, the total number of sequences was dramatically lower, suggestive of abnormal peripheral proliferation (Fig. 4c).

In addition, we calculated the various TRGV gene usages for the unique and total sequences. TRGV10 gene usage was notable for a significantly low number of unique sequences as compared with the healthy controls. In contrast, TRGV10 gene usage showed a high number of total sequences in the patients as compared with the controls. In other TRGV gene usages, the differences were not significant (Fig. 4d).

We also suspected a link between TRGV10 gene usage and clonal expansion (Fig. 4d). To assess this, we looked specifically at the ten most prevalent clones in each patient's repertoire and found that, indeed, the large clones observed in the patients' TRG repertoire used the TRGV10 gene and accounted for a large proportion of the total sequences (Fig. 4e). Taken together, these results indicate abnormal clonal expansion specifically involving the TRGV10 gene.

Exome Sequencing Analysis, Sanger Sequencing, and Functional Activity

A homozygous recessive inheritance pattern was suspected due to the high incidence of family consanguinity. A novel bi-allelic *MALT1* missense mutation (c.1799T>A; p. I600N) was identified in P1 by WES and confirmed by direct Sanger sequencing. Direct Sanger sequencing showed that P2 had the same mutation. Segregation of the identified mutation with the disease phenotype was confirmed within both families (Fig. 1, Fig. 5a). The I600N residue was found to be highly

Table 1 Immunological work-up of the newly identified MALT-1-deficient patients

Status at presentation	P1	P2	Normal range[a]
CBC		Cells/mL × 10^{-3}	
WBC	27.7	23	5.2–11
Monocytes	1.4	1.64	0.2–1
Lymphocytes	12.8	12.6	1.5–6 5
Hemoglobin (g/dL)	8.9	7.3	11–14
Platelets	373	295	150–400
Eosinophils	4.4	0.08	0–0.7
Serum immunoglobulin		mg/dL	
IgA	< 25	< 25	38–222
IgM	25	146	56–208
IgG	177	1110	590–1430
IgE	NA[c]	< 5	0–90
T lymphocyte subsets		Cells/mm^3 × 10^{-3} (%)	Normal range[b]
Lymphocytes	21.3 (46.3)	12.7 (81.8)	2.3–5.4
T (CD3+)	11.56 (86)	10.8 (85)	1.4–3.7 (60–85)
T helper (CD4+)	6.4 (53)	3.9 (31)	0.7–2.2 (36–63)
T cytotoxic (CD8+)	3.6 (25)	6.3 (49)	0.49–1.3 (15–40)
Double-negative (CD4–CD8–CD3+αβ+)	13%	0.3%	< 1%
CD3+CD4+CD25+FOXP3+ y cell (%)	0 (0)	0 (0)	> 5%
αβ TCR (%)	74	78	58% (26–100%)
γδ TCR (%)	2	8	6% (1–38%)
B (CD 20+)	1.7 (13)	1.65 (13)	0.05–0.3 (5–25)
NK (CD16+CD56+) (%)	5	4	6–30
Th17 (%)	0.2	0.2	> 1.0%
TRECs (copies per 0.5 μg DNA)	1323	1268	> 400
B lymphocyte subsets		Cells/mm^3 × 10^{-3} (%)	Normal range[d]
Lymphocytes	NA[c]	23.0 (71.4)	2.3–5.4
B cells (CD45+CD19+)	NA[c]	2.30 (10)	0.05–0.3 (5–25)
Class switched B cells (IgM^-IgD^-CD19)	NA[c]	0.09 (3.9)	0.01–0.13 (1.1–10.1)
Naïve B cells (IgD^+CD27^- CD19)	NA[c]	1.95 (85)	0.5–0.17 (68.1–89.3)
Marginal zone B cells (IgD^+ $CD19^+CD27^+$)	NA[c]	0.08 (3.5)	0.03–0.17 (4.1–13.9)
Class switched memory B cells (IgM^-IgD^- $CD19^+CD27^+$)	NA[c]	0.036 (1.5)	0.03–0.18 (3.9–13.6)
$CD21^{low}$ B cells ($CD21^{low}$ $CD19^+CD38^-$)	NA[c]	NA[c]	0.01–0.06 (1.0–5.7)
Transitional B cells ($IgM^{++}CD19^+CD38^{++}$)	NA[c]	0.714 (31)	0.03–0.20 (3.3–16.5)

[a] Healthy donors, aged 1–2 years, with percentages/counts presented as median (10th and 90th percentiles) [44]

[b] Pediatric reference values for the peripheral T cell compartment [45]

[c] NA, non-available

[d] Reference values for evaluation of B cell maturation process in the peripheral blood [46]

evolutionary conserved (Fig. 5b). The WES did not reveal any other mutation known to be involved in immunodeficiency or immune dysregulation. This mutation, affecting a highly conserved amino acid (Fig. 5b), is predicted to be deleterious by several different bioinformatics prediction programs (SIFT, Polyphen2—HDIV, Polyphen2—HVAR, LRT, Mutation Taster AND Mutation Assessor). The variant is exceedingly rare and could not be found in gnomAD nor in our in-house cohort of 2000 Israeli exomes. CADD score of the mutation was 28.7 suggesting pathogenicity. The *MALT1* mutation is different from previously described patients (Fig. 5c). Our patients share clinical and laboratory characteristics with previously described human cases and animal models with MALT1 deficiency [9, 10, 32, 33] which supports our hypothesis that the identified homozygous *MALT1* variant is a disease-causing mutation causing loss-of-function effect. Indeed, Western blot analysis of PBMCs from P2's whole blood showed markedly reduced MALT1 protein expression,

Table 2 Lymphocyte proliferation assay—thymidine incorporation assays documented reduced T cell proliferation upon stimulation with anti-CD3, as compared to healthy control

	No stimulation (CPM)	No stimulation (SI)	CD3 (SI)	PHA25 (SI)	IL-2 (SI)	IL-2+ CD3 (SI)
P1	357	1	2.5	150	103.5	74
P2	293	1	2	331.5	103.5	154.5
Control	588	1	56.5	202.5	117.5	138

CPM, counts per minute; SI, all values of stimulation with mitogens are presented as stimulation index—number of counts per minute divided by number of counts per minute without stimulation

similar to that seen in other MALT1-deficient patients with missense mutations [7] (Fig. 6). While there is no specific domain ascribed to the region around amino acid 600, it is noteworthy that the missense mutation described by McKinnon et al. [8] which also affects protein expression is nearby at position 580. Consistent with a mutation disrupting MALT1-mediated signaling, and despite sample quality from the patient and travel control which precluded some signaling studies, CD4 T cells from the patient showed that NFκB and mTORC1 activation (measured by pS6) were impaired after short-term stimulation with PMA (Fig. 7). Furthermore, anti-CD3/CD28-mediated activation for 24 h showed poor CD25 upregulation, especially among naïve cells and a sustained defect in pS6 activation among memory cells as measured by increased side scatter size (Fig. 8).

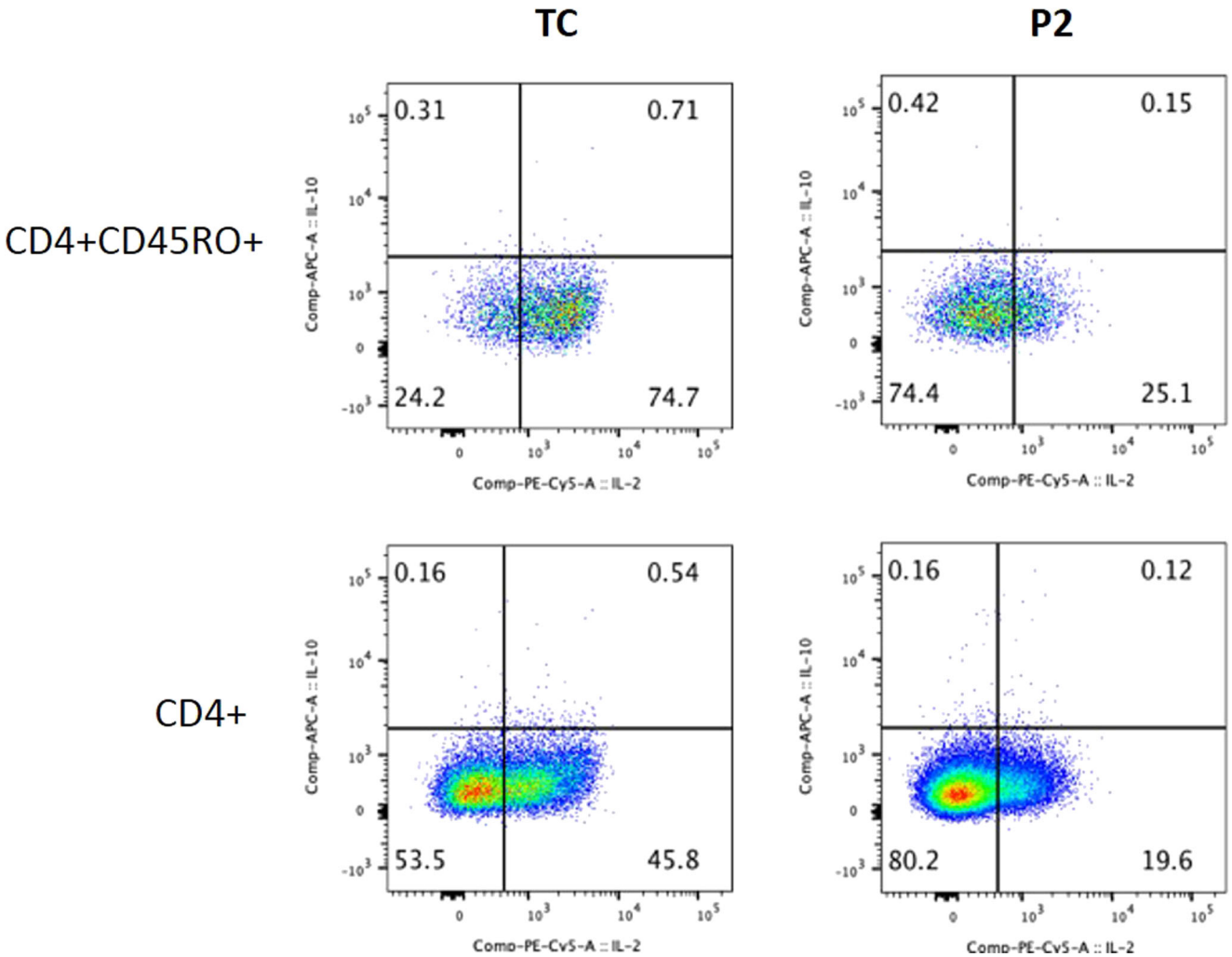

Fig. 2 Decreased IL-2 secretion in the MALT1 patient after PMA & ionomycin stimulation. Travel control (TC) and MALT1-mutated patient (P2)'s PMBCs were treated with PMA and ionomycin for 5 h in the presence of BD GolgiStop, and cytokine production was analyzed by flow cytometry

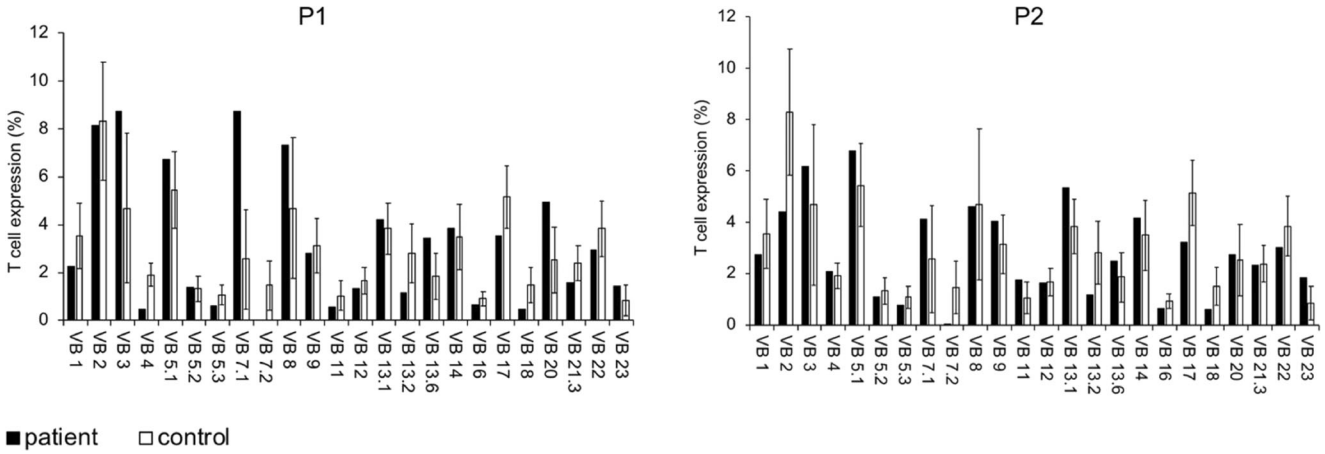

Fig. 3 T cell receptor Vβ repertoire analyses. Flow cytometry analysis of surface membrane expression of 24 T cell receptor β chain's variable gene families, in our two MALT1-deficient patients (black bars), compared with the healthy controls (white bars)

Discussion

Mutation in MALT1 was first described in association with a B cell lymphoma of the gastrointestinal tract [34]. Chromosomal translocations of another protein, BCL10, were later shown to be associated with this type of lymphoma as well [35]. The connection between these two proteins was further elucidated with the discovery that, together with CARD11 [36], they form the CBM intracellular complex that mediates NFκB activation [37]. Somatic gain-of-function (GOF) mutations involving genes comprising this complex lead to the constitutive activation of NFκB signaling,

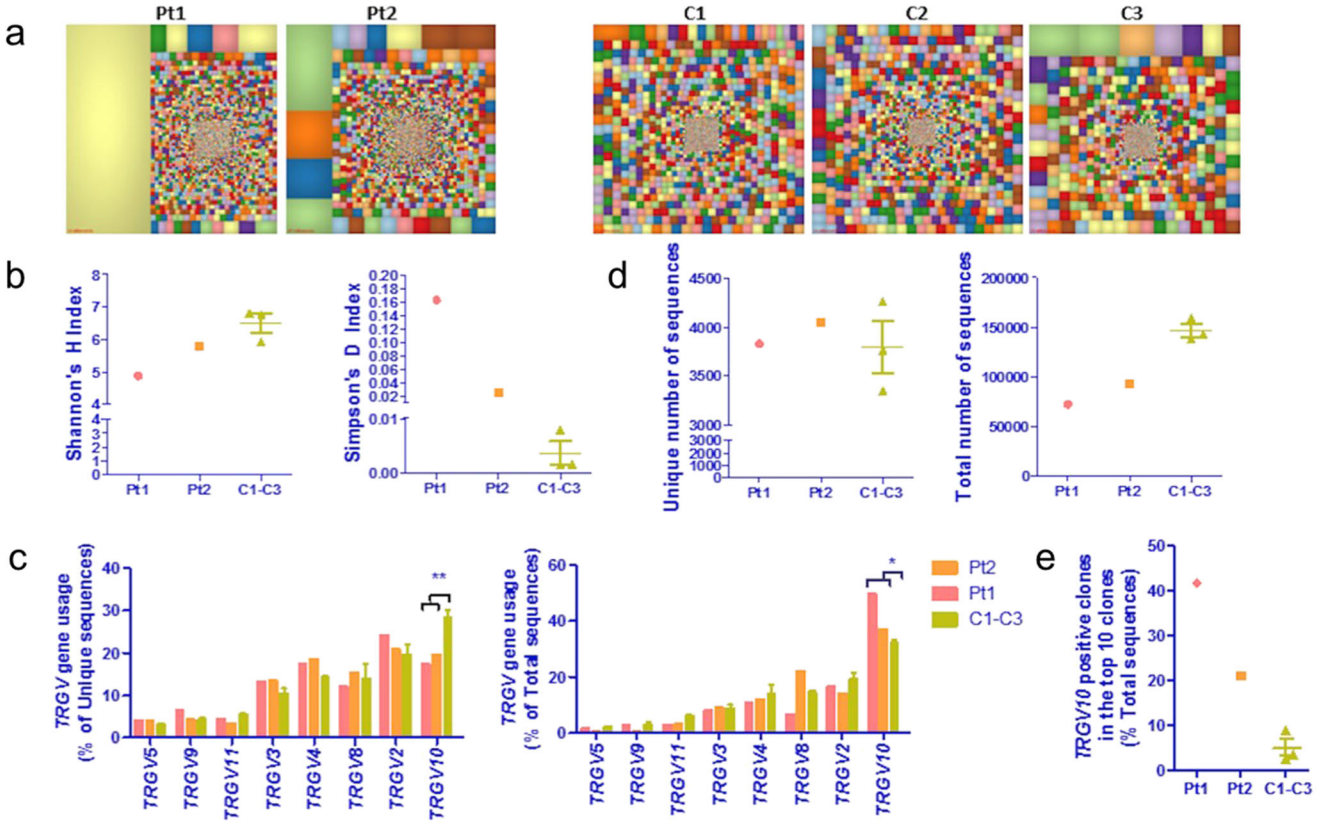

Fig. 4 Characteristics of the TRG repertoire determined by NGS. **a** Graphical presentation of the TRG repertoire using Tree map program where each square represents a specific clone and the size of each square represents the frequency of the clone within the repertoire. **b** Shannon's H diversity index and Simpson's index of unevenness. **c** The number of unique and total sequences for the patients and healthy controls ($n = 3$). **d** Bar graphs representing the percent of TRGV gene usages of the unique and total sequences (one-tail t test; * for $0.05 > p > 0.01$; ** for $0.01 > p > 0.001$). **e** Percent of total sequences for the top 10 *TRGV10* positive clones (P1, patient 1; P2, patient 2; C1–C3, healthy controls)

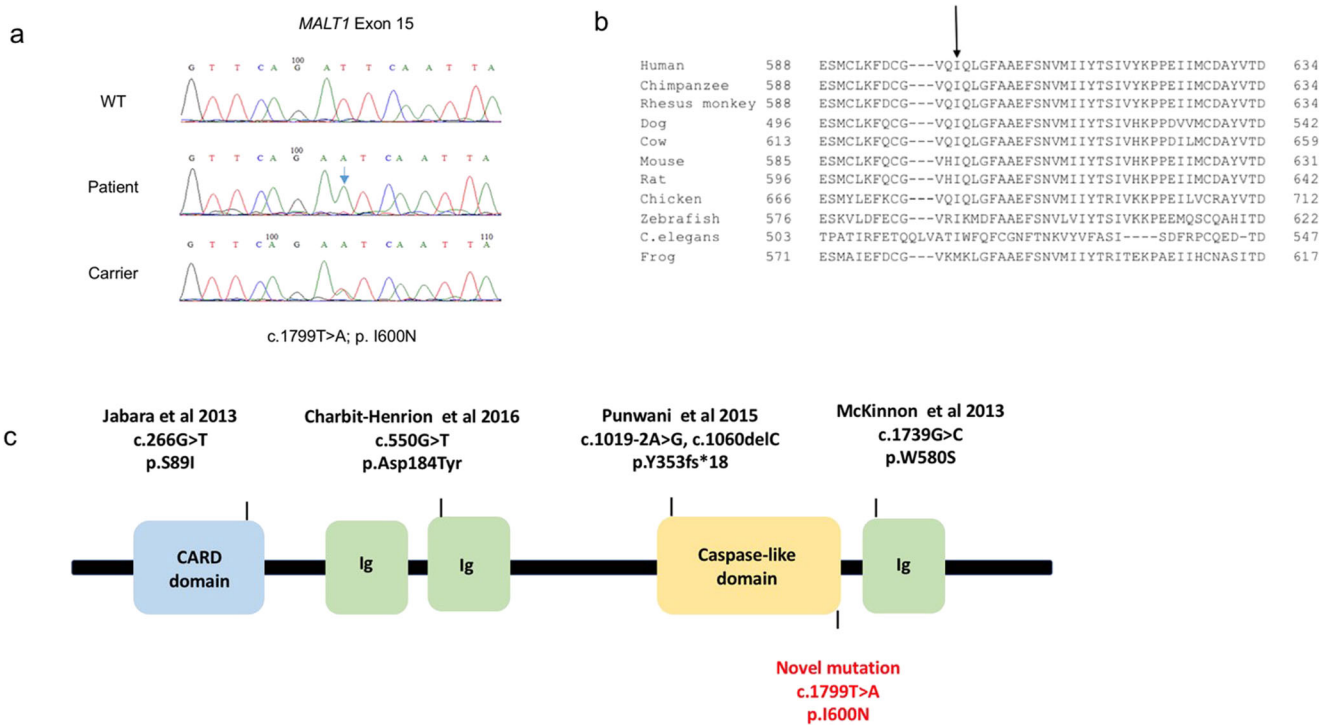

Fig. 5 Validation of MALT1 mutation. **a** Sanger sequencing confirmed the presence of a mutation (c.1799T>A; p. I600N) in peripheral blood mononuclear cells of both patients (PBMCs). A heterozygous state was found for P1's mother and two out of three of his siblings. **b** Evolutionary conservation of the mutated I600N residue among different species. **c** MALT1 protein structure and position of current and previously described mutations [7–10]

lympho-proliferation, and development of lymphoma [38]. Loss of function of the CBM proteins impairs immune function in a variety of ways [39]. Recent reviews by Lu et al. [15] and Juilland and Thome [16] explore the different immunodeficiency syndromes associated with mutations in CBM genes. These reviews emphasize the dual role of MALT1 in activation of NFκB, both in scaffolding and in protease activity, and different mutations may cause different disease phenotypes, as suggested by the data of animal models. When comparing MALT1 knock-out mice (*Malt1*$^{-/-}$) and MALT1 paracaspase mutated mice (*Malt1*$^{PD/PD}$) [32], a different phenotype is observed with a more immunocompromised picture in the former and a more auto-inflammatory presentation in the latter.

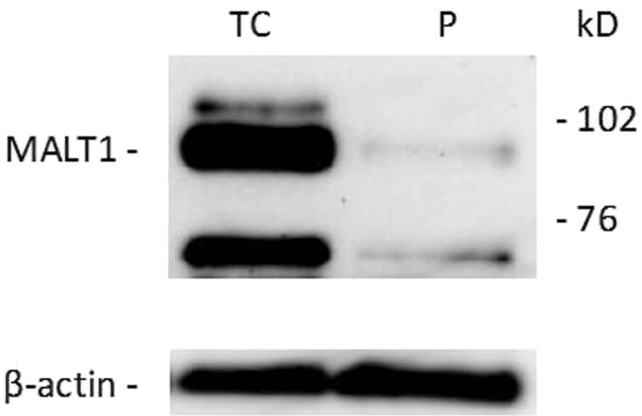

Fig. 6 P2's MALT1 protein expression markedly reduced. MALT1 protein from the total PBMCs of whole blood was detected by Western blot analysis using a MALT1 rabbit polyclonal antibody and β-actin as loading control. TC, travel control. Molecular weight (M.W.) of MALT1 is about 90 kD

To date, only six patients with immune deficiency resulting from bi-allelic mutations in *MALT1* have been reported [7–10]. All six suffered from recurrent bacterial, viral, and fungi infections, eczema, enteropathy, periodontal disease, and failure to thrive. Several had dysmorphic features [8–10]. Except for one patient [9], all patients were born to consanguineous families. All, but one, of these patients had a missense mutation of the *MALT1* gene; the other had a compound bi-allelic mutation [9]. The six patients were all noted to have evidence of immune dysregulation with poor specific antibody response to vaccines and decreased T cell proliferative responses to mitogens. Several patients demonstrated decreased expression of IL-2 [9, 10]; another demonstrated B cell lymphopenia combined with a defect in normal B cell maturation. Levels of regulatory T cells were assessed and were low in several reports [9, 10]. In several patients, there was evidence of reduced MALT1 protein expression and defect in the canonical NFκB signaling [8–10].

In this article, we describe two related patients with a novel *MALT1* homozygous mutation (p.I600N). They share clinical

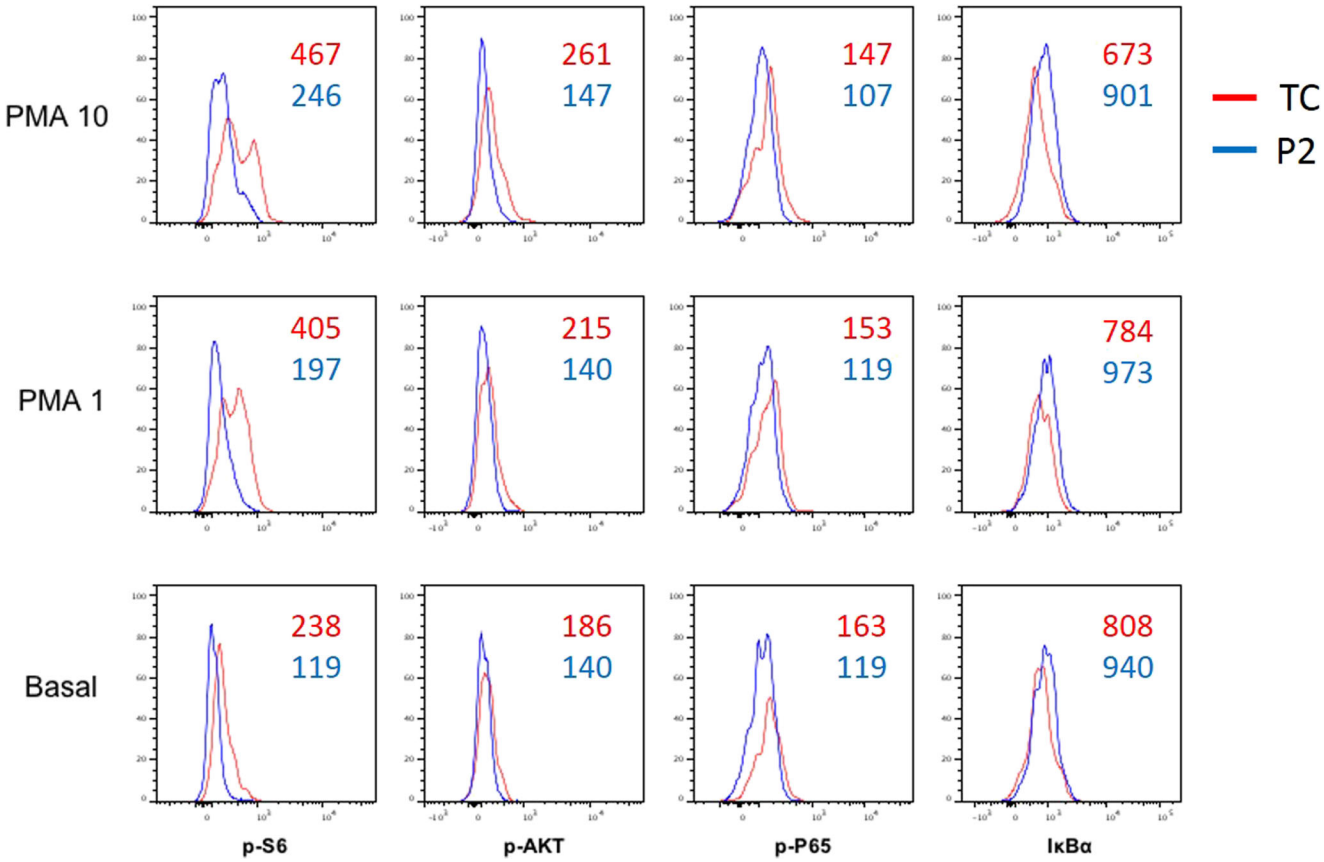

Fig. 7 mTOR and NFκB signaling pathway in MALT1 patient. Activation of (CD3+CD8−) T cells signaling molecule after 20 min of PMA stimulation analyzed by flow cytometry demonstrates decreased signaling in *MALT1* patient compared with the healthy control (PMA1: 1 ng/mL, PMA10: 10 ng/mL). Numbers indicate the mean fluorescence intensity (MFI), Travel control (TC) and Patient (P2)

and immunological features suggestive of lymphoproliferation and autoimmunity, in addition to increased susceptibility to viral and bacterial infections, dermatitis, recurrent aphthous oral lesions, and failure to thrive. Additional clinical features included dysmorphic features, hypertrichosis, and lymphoproliferation with prominent generalized lymphadenopathy. These patients also showed clinical signs of autoimmunity with manifestations such as alopecia areata and vitiligo. The immunologic profile demonstrated impaired humoral immunity in P1, a feature common to all the previously described patients, and an impaired proliferative response to specific mitogen stimulations. Both of our patients had decreased lymphocyte proliferation following anti-CD3 stimulation, which was improved in vitro, *with* exogenous IL-2 addition (Table 2). This finding, along with reduced IL-2 production, has been noted in previous studies [7, 10] and suggests that MALT1 mutations may lead to abnormal production of IL-2, a critical cytokine in T cell proliferation.

Profiling the TCR repertoire using NGS revealed a diverse repertoire but with an obvious abnormal clonal expansion pattern. Notably, the more commonly used TCR Vβ assay failed to detect these abnormalities. Both the Shannon's H diversity and the Simpson's D indices showed that the repertoire of P1 is more adversely affected than that of P2, which correlates with the more severe phenotype of P1. The number of unique sequences of the patients' TRG repertoires was similar to those of healthy controls; however, the number of total sequences was significantly lower. This is significant as it suggests that the problem arises not in the thymus but in the peripheral proliferation of T cells (especially γδT cells). The finding that there is clonal expansion of γδT cells in the peripheral blood of these patients merits further study. It is crucial to determine the nature and source of these expanded clones and whether they are present in the affected skin lesions and/or gastro-intestinal biopsies. Our study of the *TRG* repertoire, as determined by NGS, demonstrates a skewed repertoire, driven by a breakdown in the regulation of peripheral adaptive immunity. Additionally, TCR activation defects were detected in P2 consistent with defects in the CBM complex. It is notable that several phenotypes which can be seen in MALT1 deficiency, including atopy, sinopulmonary infection, and viral infection, can also be seen in patients with dominant-negative CARD11 mutations [23, 40, 41]. Similar to CARD11 mutant patients, the MALT1 mutant patient had a defect in mTORC1 activation, which had not previously been examined in MALT1 mutant

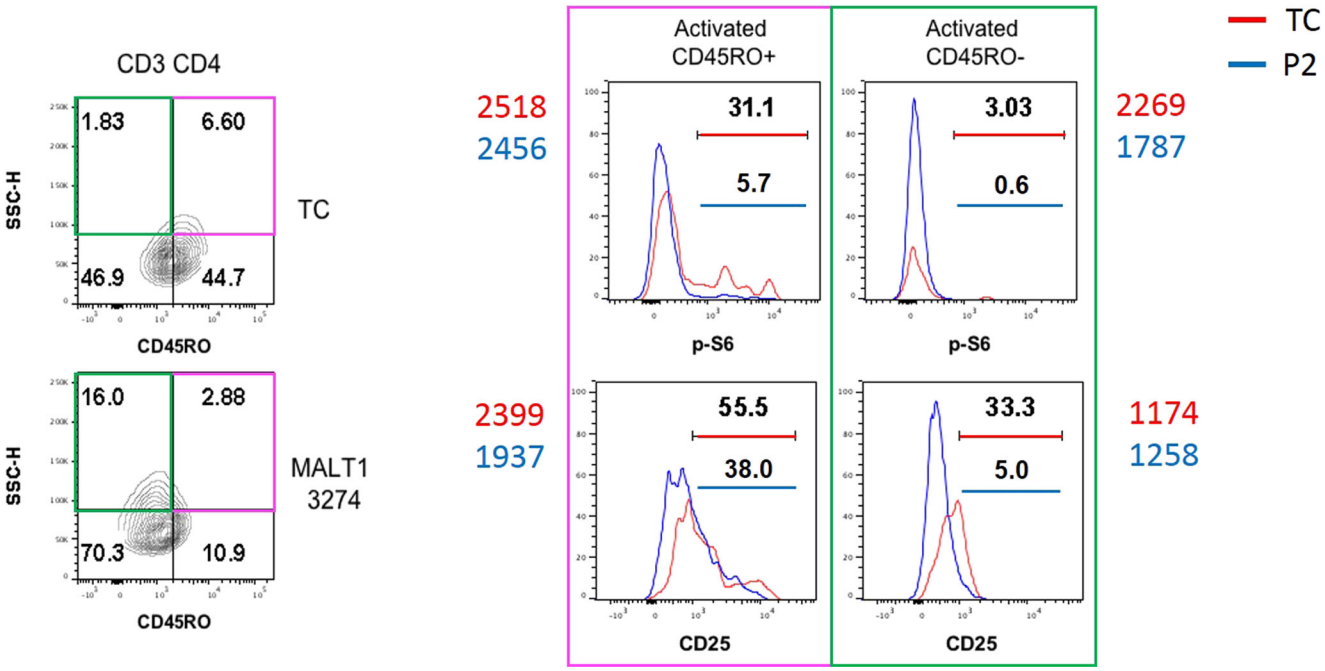

Fig. 8 Phosphorylation in activated CD4$^+$ cells in MALT1 patient. **a** Live CD4$^+$ cells were gated on CD45RO and SSC-H to indicate activated memory (purple box) and naïve (green box) cells. **b** phospho-S6 and CD25 inductions were measured in control (red) and P2 (blue) in activated memory (purple box) and naïve (green box) populations after incubating the PBMCs in plate-bound anti-CD3 plus anti-CD28 for 24 h. Decreased inductions were observed in the activated CD4$^+$ cells of the MALT1 patient after anti-CD3/CD28 stimulation, compared with the healthy control. Numbers indicate the mean fluorescence intensity (MFI)

patients. Whether the allergic disease in MALT1 and CARD11 mutant patients is directly attributable to the mTORC1 activation defect is a matter of current study, but the results presented here suggest that glutamine supplementation, which was able to restore defects in the CARD11 mutant patient cells, might be a therapeutic option for some of the symptoms in MALT1 deficiency.

MALT1 deficienct patients have substantial heterogeneity of severity and phenotypes, even within families, as do the two cousins reported here. P1 currently exhibits a more severe phenotype that seems closer to the phenotype displayed by the animal model of *Malt1* protease deficient/protease dead mice [32, 42]. These mice display severe inflammation with additional characteristics of lymphadenopathy and neurodegeneration. They have highly elevated serum concentrations of the inflammatory cytokines, such as IFNγ, and reduced levels of anti-inflammatory cytokines, such as IL-10 and TNF-α [42, 43]. In addition, severe impairment in regulatory T cells may contribute to the development of autoimmunity [32]. The clinical discrepancies between the phenotype of the cousins might be related to disease progression over time, other modifying genetic changes, and other environmental factors that may affect the phenotype. Currently, both patients continue to suffer from recurrent infections despite prophylactic treatment with IVIG replacement therapy and antibiotic prophylaxis while they await HSCT. Of the six patients previously reported, two died in the first two decades of life due to overwhelming infection [7], while the remaining four underwent successful HSCT with a reduced intensity conditioning protocol. Based on the severity of the disease, HSCT is the preferred treatment in most patients as it is the only curative treatment option in MALT1 deficiency.

Conclusion

MALT1 deficiency is a rare immunodeficiency syndrome of the NFκB pathway, characterized by early onset of a combined immune deficiency with severe life-threatening infections and autoimmune manifestations. The immunologic profile of affected patients includes humoral deficiency with either hypogammaglobulinemia or dysgammaglobulinemia, poor specific antibody responses to vaccines, normal to absent regulatory T cell numbers, low levels of Th17 cells, and decreased IL2 production in vitro. Our two newly diagnosed patients have a novel mutation in the *MALT1* gene, further linking this gene to a specific inborn error of immunity. Our investigation of these patients extends and further supports the clinical and immunological data regarding the spectrum of MALT1 deficiency and provides new insight into this primary immunodeficiency. Due to the severity of the syndrome, HSCT is the preferred treatment modality.

Acknowledgements The authors thank the patients and their families for their collaboration and the expert care by the interdisciplinary pediatric teams. Raz Somech is supported by grants from the Jeffrey Modell Foundation (JMF) and the Israeli Science Foundation (ISF). The authors would like to acknowledge Dr. Abigail Lazar for editing the manuscript.

Compliance with Ethical Standards

Conflict of Interest The authors declared that they have no conflict of interest.

References

1. Tasher D, Dalal I. The genetic basis of severe combined immunodeficiency and its variants. Appl Clin Genet. 2012;5:67–80.
2. Somech R, Roifman CM. Mutation analysis should be performed to rule out gammac deficiency in children with functional severe combined immune deficiency despite apparently normal immunologic tests. J Pediatr. 2005;147(4):555–7.
3. Picard C, Al-Herz W, Bousfiha A, Casanova JL, Chatila T, Conley ME, et al. Primary immunodeficiency diseases: an update on the Classification from the International Union of Immunological Societies Expert Committee for Primary Immunodeficiency 2015. J Clin Immunol. 2015;35(8):696–726.
4. Roifman CM, Somech R, Kavadas F, Pires L, Nahum A, Dalal I, et al. Defining combined immunodeficiency. J Allergy Clin Immunol. 2012;130(1):177–83.
5. Speckmann C, Doerken S, Aiuti A, Albert MH, Al-Herz W, Allende LM, et al. A prospective study on the natural history of patients with profound combined immunodeficiency: an interim analysis. J Allergy Clin Immunol. 2017;139(4):1302–10 e4.
6. Akar HH, Patiroglu T, Hershfield M, van der Burg M. Combined immunodeficiencies: twenty years experience from a single center in Turkey. Cent Eur J Immunol. 2016;41(1):107–15.
7. Jabara HH, Ohsumi T, Chou J, Massaad MJ, Benson H, Megarbane A, et al. A homozygous mucosa-associated lymphoid tissue 1 (MALT1) mutation in a family with combined immunodeficiency. J Allergy Clin Immunol. 2013;132(1):151–8.
8. McKinnon ML, Rozmus J, Fung SY, Hirschfeld AF, Del Bel KL, Thomas L, et al. Combined immunodeficiency associated with homozygous MALT1 mutations. J Allergy Clin Immunol. 2014;133(5):1458–62 62 e1–7.
9. Punwani D, Wang H, Chan AY, Cowan MJ, Mallott J, Sunderam U, et al. Combined immunodeficiency due to MALT1 mutations, treated by hematopoietic cell transplantation. J Clin Immunol. 2015;35(2):135–46.
10. Charbit-Henrion F, Jeverica AK, Begue B, Markelj G, Parlato M, Avcin SL, et al. Deficiency in mucosa-associated lymphoid tissue lymphoma translocation 1: a novel cause of IPEX-like syndrome. J Pediatr Gastroenterol Nutr. 2017;64(3):378–84.
11. Ruland J, Duncan GS, Wakeham A, Mak TW. Differential requirement for Malt1 in T and B cell antigen receptor signaling. Immunity. 2003;19(5):749–58.
12. Thome M. CARMA1, BCL-10 and MALT1 in lymphocyte development and activation. Nat Rev Immunol. 2004;4(5):348–59.
13. Thome M. Multifunctional roles for MALT1 in T-cell activation. Nat Rev Immunol. 2008;8(7):495–500.
14. Thome M, Charton JE, Pelzer C, Hailfinger S. Antigen receptor signaling to NF-kappaB via CARMA1, BCL10, and MALT1. Cold Spring Harb Perspect Biol. 2010;2(9):a003004.
15. Lu HY, Bauman BM, Arjunaraja S, Dorjbal B, Milner JD, Snow AL, et al. The CBM-opathies—a rapidly expanding spectrum of human inborn errors of immunity caused by mutations in the CARD11-BCL10-MALT1 complex. Front Immunol. 2018;9:2078.
16. Juilland M, Thome M. Holding all the CARDs: how MALT1 controls CARMA/CARD-dependent signaling. Front Immunol. 2018;9:1927.
17. Hamilton KS, Phong B, Corey C, Cheng J, Gorentla B, Zhong X, et al. T cell receptor-dependent activation of mTOR signaling in T cells is mediated by Carma1 and MALT1, but not Bcl10. Sci Signal. 2014;7(329):ra55.
18. E A, P D, MP L, V G. IMGT((R)) tools for the nucleotide analysis of immunoglobulin (IG) and T cell receptor (TR) V-(D)-J repertoires, polymorphisms, and IG mutations: IMGT/V-QUEST and IMGT/HighV-QUEST for NGS. Methods Mol Biol. 2012;882:569–604.
19. CJ K. Simpson diversity and the Shannon–Wiener index as special cases of a generalized entropy. Oikos. 2005;109:203–7.
20. Li H, Durbin R. Fast and accurate long-read alignment with Burrows-Wheeler transform. Bioinformatics. 2010;26(5):589–95.
21. McKenna A, Hanna M, Banks E, Sivachenko A, Cibulskis K, Kernytsky A, et al. The genome analysis toolkit: a MapReduce framework for analyzing next-generation DNA sequencing data. Genome Res. 2010;20(9):1297–303.
22. Li MX, Gui HS, Kwan JS, Bao SY, Sham PC. A comprehensive framework for prioritizing variants in exome sequencing studies of Mendelian diseases. Nucleic Acids Res. 2012;40(7):e53.
23. Ma CA, Stinson JR, Zhang Y, Abbott JK, Weinreich MA, Hauk PJ, et al. Germline hypomorphic CARD11 mutations in severe atopic disease. Nat Genet. 2017;49(8):1192–201.
24. Sufficool KE, Lockwood CM, Abel HJ, Hagemann IS, Schumacher JA, Kelley TW, et al. T-cell clonality assessment by next-generation sequencing improves detection sensitivity in mycosis fungoides. J Am Acad Dermatol. 2015;73(2):228–36 e2.
25. Kansal R, Grody WW, Zhou J, Dong L, Li X. The value of T-cell receptor gamma (TRG) clonality evaluation by next-generation sequencing in clinical hematolymphoid tissues: a descriptive study of 41 cases from a single institution. Am J Clin Pathol. 2018;150:193–223.
26. Mahe E, Pugh T, Kamel-Reid S. T cell clonality assessment: past, present and future. J Clin Pathol. 2018;71(3):195–200.
27. Cruz MS, Diamond A, Russell A, Jameson JM. Human alphabeta and gammadelta T cells in skin immunity and disease. Front Immunol. 2018;9:1304.
28. Johnston EL, Roberts DA. Contaminants reduce the richness and evenness of marine communities: a review and meta-analysis. Environ Pollut. 2009;157(6):1745–52.
29. Simpson EH. Measurement of diversity. Nature. 1949;163:688.
30. Rechavi E, Lev A, Lee YN, Simon AJ, Yinon Y, Lipitz S, et al. Timely and spatially regulated maturation of B and T cell repertoire during human fetal development. Sci Transl Med. 2015;7(276):276ra25.
31. Lee YN, Frugoni F, Dobbs K, Tirosh I, Du L, Ververs FA, et al. Characterization of T and B cell repertoire diversity in patients with RAG deficiency. Sci Immunol. 2016;1(6):eaah6109.
32. Bornancin F, Renner F, Touil R, Sic H, Kolb Y, Touil-Allaoui I, et al. Deficiency of MALT1 paracaspase activity results in unbalanced regulatory and effector T and B cell responses leading to multiorgan inflammation. J Immunol. 2015;194(8):3723–34.
33. Ruefli-Brasse AA, French DM, Dixit VM. Regulation of NF-kappaB-dependent lymphocyte activation and development by paracaspase. Science. 2003;302(5650):1581–4.
34. Isaacson P, Wright DH. Malignant lymphoma of mucosa-associated lymphoid tissue. A distinctive type of B-cell lymphoma. Cancer. 1983;52(8):1410–6.
35. Willis TG, Jadayel DM, Du MQ, Peng H, Perry AR, Abdul-Rauf M, et al. Bcl10 is involved in t(1;14)(p22;q32) of MALT B cell

lymphoma and mutated in multiple tumor types. Cell. 1999;96(1):35–45.
36. Sommer K, Guo B, Pomerantz JL, Bandaranayake AD, Moreno-Garcia ME, Ovechkina YL, et al. Phosphorylation of the CARMA1 linker controls NF-kappaB activation. Immunity. 2005;23(6):561–74.
37. Lucas PC, Yonezumi M, Inohara N, McAllister-Lucas LM, Abazeed ME, Chen FF, et al. Bcl10 and MALT1, independent targets of chromosomal translocation in malt lymphoma, cooperate in a novel NF-kappa B signaling pathway. J Biol Chem. 2001;276(22):19012–9.
38. Juilland M, Thome M. Role of the CARMA1/BCL10/MALT1 complex in lymphoid malignancies. Curr Opin Hematol. 2016;23(4):402–9.
39. Perez de Diego R. Immunodeficiency and CARD-BCL10-MALT1. Oncotarget. 2015;6(24):19934–5.
40. Dadi H, Jones TA, Merico D, Sharfe N, Ovadia A, Schejter Y, et al. Combined immunodeficiency and atopy caused by a dominant negative mutation in caspase activation and recruitment domain family member 11 (CARD11). J Allergy Clin Immunol. 2018;141(5):1818–30 e2.
41. Dorjbal B, Stinson JR, Ma CA, Weinreich MA, Miraghazadeh B, Hartberger JM, et al. Hypomorphic caspase activation and recruitment domain 11 (CARD11) mutations associated with diverse immunologic phenotypes with or without atopic disease. J Allergy Clin Immunol. 2018.
42. Yu JW, Hoffman S, Beal AM, Dykon A, Ringenberg MA, Hughes AC, et al. MALT1 protease activity is required for innate and adaptive immune responses. PLoS One. 2015;10(5):e0127083.
43. Gewies A, Gorka O, Bergmann H, Pechloff K, Petermann F, Jeltsch KM, et al. Uncoupling Malt1 threshold function from paracaspase activity results in destructive autoimmune inflammation. Cell Rep. 2014;9(4):1292–305.
44. Shearer WT, Rosenblatt HM, Gelman RS, Oyomopito R, Plaeger S, Stiehm ER, et al. Lymphocyte subsets in healthy children from birth through 18 years of age: the Pediatric AIDS Clinical Trials Group P1009 study. J Allergy Clin Immunol. 2003;112(5):973–80.
45. Schatorje EJ, Gemen EF, Driessen GJ, Leuvenink J, van Hout RW, de Vries E. Paediatric reference values for the peripheral T cell compartment. Scand J Immunol. 2012;75(4):436–44.
46. Piatosa B, Wolska-Kusnierz B, Pac M, Siewiera K, Galkowska E, Bernatowska E. B cell subsets in healthy children: reference values for evaluation of B cell maturation process in peripheral blood. Cytometry B Clin Cytom. 2010;78(6):372–81.